Pis'ma v ZhETF, vol.68, iss.12, pp.870 - 875

ORBITAL MAGNETISM IN SMALL QUANTUM DOTS WITH CLOSED SHELLS

*W.D.Heiss**, *R.G.Nazmitdinov**†

**Centre for Nonlinear Studies and Department of Physics, University of the Witwatersrand, Johannesburg, South Africa*

†*Joint Institute for Nuclear Research, 141980 Dubna, Russia*

Submitted 10 November 1998

It is found that various kind of shell structure which occurs at specific values of the magnetic field leads to the disappearance of the orbital magnetization for particular magic numbers of small quantum dots with an electron number $A < 30$.

PACS: 73.20.Dx, 73.23.Ps

The development of semiconductor technology has made possible the confinement of a finite number of electrons in a localized space of a few hundred Angstroms [1]. These mesoscopic systems called quantum dots open new avenues in the study of the interplay between quantum and classical behavior at a low-dimensional scale. The smaller the quantum dot, the larger the prevalence of quantum effects upon the static and dynamic properties of the system. Their electronic properties are determined by the interplay of the external confinement and the electron-electron interaction which produces the effective mean field of the "artificial atom" [2, 3].

The quasiparticle concept associated with an effective mean field is well established in many particle physics. For finite Fermi system like nuclei or metallic clusters the bunching of single particle levels known as shells [4, 5] is one consequence of this description, if the mean free path of the particles is comparable with the size of the system. A remarkable stability is found in nuclei and metallic clusters at magic numbers which correspond to closed shells in the effective potential. For small quantum dots, where the number of electrons is well defined ($A < 30$), the mean free path of the electrons appears to be comparable with the diameter of the dot. Transport phenomena are governed by the physics of the Coulomb blockade regime [3]. In recent experiments [6–8] shell structure effects have been observed clearly for quantum dots. In particular, the energy needed to place the extra electron (addition energy) into a vertical quantum dot at zero magnetic field has characteristic maxima which correspond to the sequence of magic numbers of a two-dimensional harmonic oscillator [7]. The energy gap between filled shells is $\hbar\omega_0$, where $\hbar\omega_0$ is the lateral confinement energy. In fact, when the confining energy is comparable to or larger than the interaction energy, these atomic-like features have been predicted in a number of publications [9–12]. While the electron-electron interaction is important for the explanation of certain ground state properties like special values of angular momenta of quantum dots in a magnetic field [2], for small number of electrons the confinement energy becomes prevalent over the Coulomb energy [9, 12, 13]. In [14] it was demonstrated that the magnetoexciton spectrum in small quantum dots resembles well the spectrum of the noninteracting electron-hole pairs. In particular, the gaps in the spectrum, which are typical features of the shell structure, reappear at different values of the magnetic field.

Recent calculations using the spin-density-functional approach [15] nicely confirm shell closure for small magic electron numbers in a parabolic quantum dot.

Orbital magnetism of an ensemble of quantum dots has been discussed for non-interacting electrons in [16–18], but little attention was paid to shell structure of an individual dot. We demonstrate within a simple model that the disappearance and re-appearance of closed shells in a quantum dot under variation of the magnetic field strength leads to a novel feature: the orbital magnetization disappears for particular values of the magnetic field strength, which are associated to particular magic numbers.

Since the electron interaction is crucial only for partially filled electronic shells [15, 19], we deal in this paper mainly with closed shells. It corresponds to the quantum limit $\hbar\omega_0 \geq e^2/\varepsilon l_0$ where $e^2/\varepsilon l_0$ is the typical Coulomb energy with $l_0 = (\hbar/m^*\omega_0)^{1/2}$, m^* is the effective electron mass and ε is the dielectric constant. In fact, for small dots, where large gaps between closed shells occur [9, 12, 14], the electron interaction plays the role of a weak perturbation which can be neglected. But even in the regime $\hbar\omega_0 < e^2/\varepsilon l_0$ a distinctively larger addition energy is needed, if an electron is added to a closed shell [15]. We choose the harmonic oscillator potential as the effective mean field for the electrons in an isolated quantum dot. Our discussion here is based upon the 2D version of the Hamiltonian [20] including spin degree of freedom. The magnetic field acts perpendicular to the plane of motion, i.e. $H = \sum_{j=1}^{A} h_j$ with

$$h = \frac{1}{2m^*}(\mathbf{p} - \frac{e}{c}\mathbf{A})^2 + \frac{m^*}{2}(\omega_x^2 x^2 + \omega_y^2 y^2) + \mu^* \sigma_z B, \tag{1}$$

where $\mathbf{A} = [\mathbf{r} \times \mathbf{B}]/2$, $\mathbf{B} = (0, 0, B)$ and σ_z is the Pauli matrix. We do not take into account the effect of finite temperature; this is appropriate for experiments which are performed at temperatures $kT \ll \Delta$ with Δ being the mean level spacing. The units used are meV for the energy and Tesla for the magnetic field strength. The effective mass is $m^* = 0.067 m_e$ for GaAs, which yields, for $A \approx 15$, the size $R_0 \approx 320\,\text{Å}$ and $\hbar\omega_0 = 3\,\text{meV}$ [20]. The effective mass determines the orbital magnetic moment for the electrons and leads to $\mu_B^{eff} = m_e/m^* \mu_B \approx 15\mu_B$. The effective spin magnetic moment is $\mu^* = g_L \mu_B$ with the effective Landé factor $g_L = 0.44$ and $\mu_B = |e|\hbar/2m_e c$. The magnetic orbital effect is much enhanced in comparison with the magnetic spin effect, yet the tiny spin splitting does produce signatures as we see below.

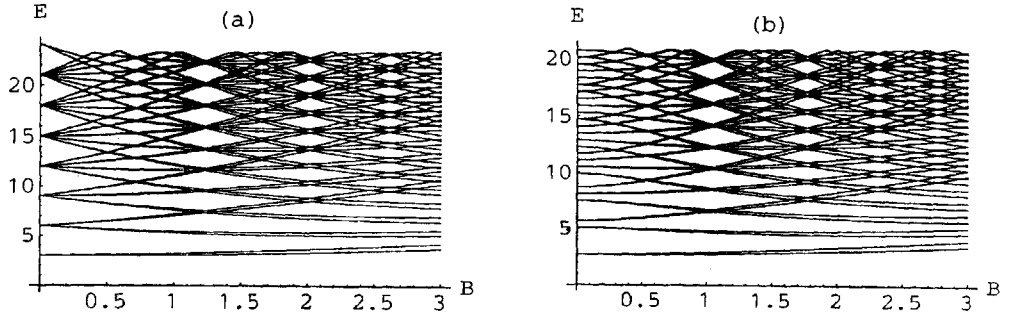

Fig.1. Single-particle spectra as a function of the magnetic field strength. Spectra are displayed for (a) a plain isotropic and (b) deformed two dimensional oscillator

Shell structure occurs whenever the ratio of the two eigenmodes $\Omega_\pm$ of the Hamiltonian (1) (see Ref.[20])

$$\Omega_\pm^2 = \frac{1}{2}(\omega_x^2 + \omega_y^2 + 4\omega_L^2 \pm \sqrt{(\omega_x^2 - \omega_y^2)^2 + 8\omega_L^2(\omega_x^2 + \omega_y^2) + 16\omega_L^4}) \qquad (2)$$

is a rational number with a small numerator and denominator. Here $\omega_L = |e|B/(2m^*c)$. Closed shells are particularly pronounced if the ratio is equal to one (for $B = 0$) or two (for $B \approx 1.23$) or three (for $B \approx 2.01$) and lesser pronounced if the ratio is $3/2$ (for $B = 0.72$) or $5/2$ (for $B = 1.65$) for a circular case $\omega_x = \omega_y$ (see Fig.1a). Note that, for better illustration, we used for the spin splitting the value $2\mu_B$ instead of the correct μ^* in all Figures; the discussions and conclusions are based on the correct value. The values given here for B depend on m^* and $\omega_{x,y}$. As a consequence, a material with an even smaller effective mass m^* would show these effects for a correspondingly smaller magnetic field. For $B = 0$ the magic numbers (including spin) turn out to be the usual sequence of the two dimensional isotropic oscillator, that is 2, 6, 12, 20,... [7]. For $B \approx 1.23$ we find new shells *as if* the confining potential would be a deformed harmonic oscillator without magnetic field. The magic numbers are 2, 4, 8, 12, 18, 24,... which are just the numbers obtained from the two dimensional oscillator with $\omega_> = 2\omega_<$ ($\omega_>$ and $\omega_<$ denote the larger and smaller value of the two frequencies). Similarly, we get for $B \approx 2.01$ the magic numbers $2, 4, 6, 10, 14, 18, 24, \ldots$ which corresponds to $\omega_> = 3\omega_<$. If we start from the outset with a deformed mean field $\omega_x = (1 - \beta)\omega_y$ with $\beta > 0$, the degeneracies (closed shells) lifted at $B = 0$ re-occur at higher values for B (see Fig.2 and discussion relating to it). In Fig.1b we display an example referring to $\beta = 0.2$. The significance of this finding lies in the restoration of closed shells by the magnetic field in an isolated quantum dot that does not give rise to magic numbers at zero field strength due to deformation. We mention that the choice $\beta = 0.5$ would shift the pattern found at $B \approx 1.23$ in Fig.1a to the value $B = 0$. The relation between B and the deformation is displayed in Fig.2, where, for better illustration, $B' = \omega_L/\omega_x$ rather than B is plotted *versus* $r = \omega_x/\omega_y$. Closed shells are obtained for values of B and β which yield $\Omega_+/\Omega_- = k = 1, 2, 3, \ldots$, that is for values on the trajectories of Fig.2.

Note also the asymmetry of the curves in Fig.2: while $\omega_x/\omega_y = r$ is physically identical with $\omega_x/\omega_y = 1/r$ without magnetic field, the two deformations become distinct by the presence of a magnetic field as it establishes a direction perpendicular to the $x - y$-plane.

In [20] we have obtained various shapes of the quantum dot by energy minimization. In this context it is worth noting that at the particular values of the magnetic field, where a closed shell occurs, the energy minimum would be obtained for circular dots, if the particle number is chosen to be equal to the magic numbers. Deviations from those magic numbers usually give rise to deformed shapes at the energy minimum. To what extent these 'spontaneous' deformations actually occur (which is the Jahn−Teller effect [21]), is subject to more detailed experimental information. The far-infrared spectroscopy in a small isolated quantum dot could be a useful tool to provide pertinent data [20].

The question arises as to what extent our findings depend upon the particular choice of the mean field. The Coulomb interaction lowers the electron levels for increasing magnetic quantum number $|m|$ [2, 13]. The addition of the term $-\lambda\hbar\omega L^2$ to the Hamiltonian (1), where L is the dimensionless z-component of the angular momentum operator, mimics this effect for $\lambda > 0$ in the Coulomb blockade regime of deformed quantum dots [22]. In this way, it interpolates the single-particle spectrum between that of the oscillator and

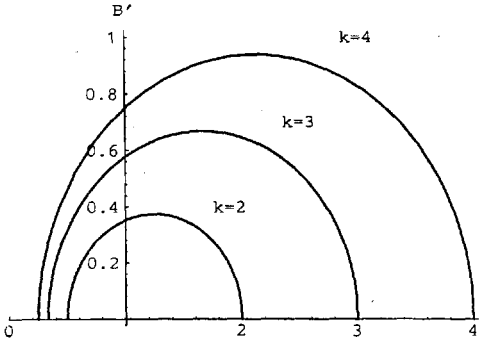

Fig.2. Relative magnetic field strength $B' = \omega_L/\omega_x$ as a function of the ratio $r = \omega_x/\omega_y = 1-\beta$ for fixed values of the ratio $k = \Omega_+/\Omega_-$

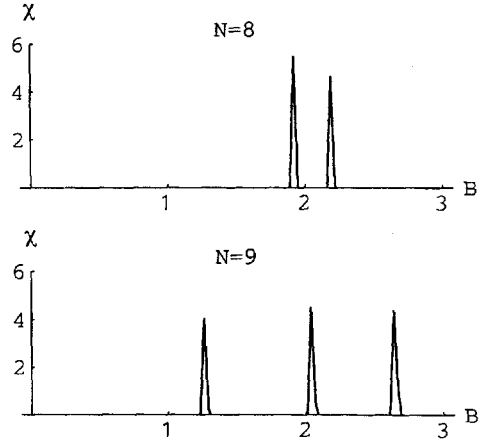

Fig.3. Magnetic susceptibility $\chi = -\partial^2 E_{\rm tot}/\partial B^2$ in arbitrary units as a function of the magnetic field strength for the isotropic oscillator without L^2-term. $E_{\rm tot}$ is the sum of the single-particle energies filled from the bottom up to the electron number A

the square well [4]. For $\omega_x \neq \omega_y$ and $\lambda \neq 0$ the Hamiltonian $H' = H - \lambda\hbar\omega L^2$ is non-integrable [23] and the level crossings encountered in Fig.1 become avoided level crossings. The shell structure, which prevails for $\lambda = 0$ throughout the spectrum at $B \approx 1.23$ or $B \approx 2.01$, is therefore disturbed to an increasing extent with increasing shell number. But even for $\lambda \leq 0.1$ the structure is still clearly discernible for about seven shells, that is for particle numbers up to about twenty five.

When the magnetic field is changed continuously for a quantum dot of fixed electron number, the ground state will undergo a rearrangement at the values of B, where level crossings occur [2, 13]. In fact, it leads to strong variations in the magnetization [2] and should be observable also in the magnetic susceptibility as it is proportional to the second derivative of the total energy with respect to the field strength. While details may be modified by electron correlations, we think that the general features discussed below should be preserved.

Fig.4. Blow-ups of the relevant level crossings explaining the features in Fig.3. The left and right hand side refers to $A = 8$ and $A = 9$, respectively

In Fig.3 we discern clearly distinct patterns depending on the electron number, in fact, the susceptibility appears to be a fingerprint pertaining to the electron number. Deforming the oscillator does not produce new features except for the fact that all lines in Fig.3 would be shifted in accordance with Fig.2. If there is no level crossing, the second derivative of $E_{\rm tot}$ is a smooth function. The crossing of two occupied levels does not change the smoothness. In contrast, if an unoccupied level crosses the last occupied level, the second derivative of $E_{\rm tot}$ must show a spike. In this way, we understand the even-odd effect when comparing $A = 8$ with $A = 9$ in Fig.3. The spin splitting caused by the magnetic field at $B \approx 2.01$ for $A = 8$ is absent for $A = 9$. This becomes evident when

looking at a blow up of this particular level crossing which is illustrated in Fig.4, where the last occupied level is indicated as a thick line and the points where a spike occurs are indicated by a dot. Note that the splitting is proportional to the effective spin magnetic moment μ^*.

Spikes of the susceptibility are associated with a spin flip for even electron numbers. They are brought about by the crossing of the top (bottom) with the bottom (top) line of a double line. Hence, both lines of the double splitting in Fig.3 yield a spin flip ($A = 8$), but neither of the single lines ($A = 9$). Strictly speaking, the spikes are δ-functions with a factor which is determined by the angle at which the two relevant lines cross. If the level crossings are replaced by avoided crossings (Landau – Zener crossings), the lines would be broadened. This would be the case in the present model for $\lambda > 0$ *and* $\beta > 0$. Finite temperature will also result in line broadening.

We now focus on the special cases which give rise to closed shells, that is when the ratio $\Omega_+/\Omega_- = k = 1, 2, 3, \ldots$ For the sake of clarity we analyze in detail the circular shape ($\omega_x = \omega_y = \omega_0$) for which the eigenmodes (Eq.(2)) become $\Omega_\pm = (\Omega \pm \omega_L)$ with $\Omega = \sqrt{\omega_0^2 + \omega_L^2}$ [24]. We find for the magnetization

$$M = \mu_B^{eff}(1 - \frac{\omega_L}{\Omega})(\sum\nolimits_- - k\sum\nolimits_+) - \mu^* < S_z > \qquad (3)$$

with $\sum_\pm = \sum_j^A (n_\pm + 1/2)_j$ [20]. For completely filled shell $< S_z >= 0$, since, for the magnetic field strengths considered here, the spin orientations cancel each other (see Fig.1). From the orbital motion we obtain for the susceptibility

$$\chi = dM/dB = -\frac{\mu_B^{eff\,2}}{\hbar\Omega}(\frac{\omega_0}{\Omega})^2(\sum\nolimits_+ + \sum\nolimits_-). \qquad (4)$$

It follows from Eq.(4) that, for a completely filled shell, the magnetization owing to the orbital motion leads to diamagnetic behavior. For zero magnetic field ($k = 1$) the system is paramagnetic and the magnetization vanishes ($\sum_- = \sum_+$). The value $k = 2$ is attained at $B \approx 1.23$. When calculating $\sum_-$ and $\sum_+$ we have to distinguish between the cases, where the shell number N of the last filled shell is even or odd. With all shells filled from the bottom we find (i) for the last filled shell number even:

$$\sum\nolimits_+ = \frac{1}{12}(N+2)[(N+2)^2 + 2], \quad \sum\nolimits_- = \frac{1}{6}(N+1)(N+2)(N+3)$$

which implies

$$M = -\mu_B^{eff}(1 - \omega_L/\Omega)(N+2)/2;$$

and (ii) for the last filled shell number odd:

$$\sum\nolimits_+ = \frac{1}{2}\sum\nolimits_- = \frac{1}{12}(N+1)(N+2)(N+3)$$

which, in turn, implies $M = 0$. Therefore, if $\Omega_+/\Omega_- = 2$, the orbital magnetization vanishes for the magic numbers $4, 12, 24, \ldots$ while it leads to diamagnetism for the magic numbers $2, 8, 18, \ldots$ A similar picture is obtained for $\Omega_+/\Omega_- = 3$ which happens at $B \approx 2.01$: for each third filled shell number (magic numbers $6, 18, \ldots$) the magnetization is zero. Since the results presented are due to shell effects, they do not depend on the assumption $\omega_x/\omega_y = 1$ which was made to facilitate the discussion. The crucial point is

the relation $\Omega_+/\Omega_- = k = 1, 2, 3, \ldots$ which can be obtained for a variety of combinations of the magnetic field strength and the ratio ω_x/ω_y as is illustrated in Fig.2. Whenever the appropriate combination of field strength and deformation is chosen to yield, say, $k = 2$, our findings apply.

To summarize: the consequences of shell structure effects for the addition energy of a small isolated quantum dot have been analyzed. At certain values of the magnetic field strength closed shells appear in a quantum dot, also in cases where deformation does not give rise to magic numbers at zero field strength. Measurements of the magnetic susceptibility are expected to reflect the properties of the single-particle spectrum and should display characteristic patterns depending on the particle number. At certain values of the magnetic field and electron numbers the orbital magnetization vanishes due to shell closure in the quantum dot.

---

1. M.A.Kastner, Phys. Today **46**, 24 (1993); R.C.Ashoori, Nature (London) **379**, 413 (1996).
2. P.A.Maksym and T.Chakraborty, Phys. Rev. Lett. **65**, 108 (1990); Phys. Rev. **B45**, 1947 (1992); M.Wagner, U.Merkt, and A.V.Chaplik, Phys. Rev. **B45**, 1951 (1992); P.Hawrylak, Phys. Rev. Lett. **71**, 3347 (1993).
3. L.P.Kouwenhoven et al, *Mesoscopic Electron Transport, Proc. of the NATO ASI* Eds. L.P.Kouwenhoven, G. Schön, and L.L.Sohn, (Series **E345**, Kluwer, Dordrecht, Netherlands, 1997, p.105.
4. S.G.Nilsson and I.Ragnarsson, *Shapes and Shells in Nuclear Structure*, Cambridge, Cambridge University Press 1995.
5. W.A. de Heer, Rev. Mod. Phys. **65**, 611 (1993); M.Brack, Rev. Mod. Phys. **65**, 677 (1993).
6. D.J.Lockwood, P.Hawrylak, P.D.Wang et al., Phys. Rev. Lett. **77**, 354 (1996).
7. S.Tarucha, D.G.Austing, T.Honda et al., Phys. Rev. Lett. **77**, 3613 (1996).
8. M.Fricke et al., Europ. Lett. **36**, 197 (1996).
9. M.Macucci, K.Hess, and G.J.Iafrate, Phys. Rev. **B48**, 17354 (1993); J. App. Phys. **77**, 3267 (1995).
10. P.A.Maksym, Phys. Rev. **B53**, 10871 (1996).
11. W.D.Heiss and R.G.Nazmitdinov, Phys. Lett. **A222**, 309 (1996).
12. M.Stopa, Phys. Rev. **B54**, 13767 (1996).
13. M.Dineykhan and R.G.Nazmitdinov, Phys. Rev. **B55**, 13707 (1997).
14. A.Wojs, P.Hawrylak, S.Fafard, and L.Jacak, Phys. Rev. **B54**, 5604 (1996).
15. K.Hirose and N.S.Wingreen, cond-mat/9808193.
16. B.L.Altshuler, Y.Gefen, and Y.Imry, Phys. Rev. Lett. **66**, 88 (1991); B.L.Altshuler et al., Phys. Rev. **B47**, 10335 (1993).
17. F.V.Oppen, Phys. Rev. **B50**, 17151 (1994).
18. K.Richter, D.Ulmo, and R.Jalabert, Phys. Rep. **276**, 1 (1996).
19. A.Wojs and P.Hawrylak, Phys. Rev. **B53**, 10841 (1996); M.Eto, Jpn. J. Appl. Phys. **36**, 3924 (1997); M.Koskinen, M.Manninen, and S.M.Reimann, Phys. Rev. Lett. **79**, 1389 (1997).
20. W.D.Heiss and R.G.Nazmitdinov, Phys. Rev. **B55**, 16310 (1997).
21. H.A.Jahn and E.Teller, Proc. R. Soc. London, Sec. **A161**, 220 (1937).
22. G.Hackenbroich, W.D. Heiss, and H.A.Weidenmüller, Phys. Rev. Lett. **79**, 127 (1997).
23. W.D.Heiss and R.G.Nazmitdinov, Phys. Rev. Lett. **73**, 1235 (1994); Physica **D118**, 134 (1998).
24. V.Fock, Z.Phys. **47**, 446 (1928).